Electro-hydrodynamic numerical modelling of corona discharge

D. Cagnoni[1,2], F. Agostini[1], T. Christen[1], C. de Falco[2], N. Parolini[2], and I. Stevanović[1]

[1] ABB Switzerland Ltd., Corporate Research, CH-5405 Baden-Dättwil, Switzerland
`ivica.stevanovic@ch.abb.com`

[2] Dipartimento di Matematica "F. Brioschi", Politecnico di Milano, via Bonardi 9, 20133 Milano, Italy

Summary. Prediction of cooling by forced convection due to corona-induced ion flow in an electro-hydrodynamic (or EHD) simulation requires a reliable corona electrode model, which has to be formulated as a boundary condition (BC) to the EHD partial differential equations. We discuss and compare four different BCs in the context of finite-volume methods (FVM). It turns out that the optimum choice depends on the given physical information.

1 EHD differential and numerical model

Corona discharge refers to field induced gas ionization near an electrode, e.g., a thin wire (*emitter*), in series with the dark discharge associated with the ion drift towards counter electrodes (*collector*). The ion motion induces a drag of the neutral gas, and can be used to convection cool a heat source, which may be the collector at the same time. The associated equations consist of the Poisson equation for the electric potential ϕ, and the balance equations for the densities for ion number N_p, mass ρ, momentum $\rho\mathbf{v}$, and energy (written in terms of the temperature T). In the Boussinesq approximation, they read

$$-\nabla \cdot (\varepsilon \nabla \phi) = qN_p \tag{1}$$

$$\frac{\partial N_p}{\partial t} = -\nabla \cdot \left(\frac{\mathbf{j}}{q}\right) = -\nabla \cdot \left((b\mathbf{E}+\mathbf{v})N_p + a\nabla N_p\right) \tag{2}$$

$$\nabla \cdot \mathbf{v} = 0 \tag{3}$$

$$\frac{D\mathbf{v}}{Dt} = \nu \Delta \mathbf{v} - \nabla\left(\frac{p}{\rho} - \mathbf{g} \cdot \mathbf{x}\right) + \mathbf{f}_B + \mathbf{f}_{\text{EHD}} \tag{4}$$

$$\rho C_V \frac{DT}{Dt} = k\Delta T + \mathbf{j} \cdot \mathbf{E} - \mathbf{f}_{\text{EHD}} \cdot \mathbf{v} \tag{5}$$

where ε is the electric permittivity, q the ion charge, $\mathbf{E} = -\nabla\phi$ the electric field, b the ion mobility, a the diffusion constant, $\frac{D\bullet}{Dt} = \frac{\partial\bullet}{\partial t} + \mathbf{v} \cdot \nabla\bullet$ the material derivative for the velocity field $\mathbf{v}$, ν the viscosity, p the pressure, $\mathbf{g}$ the gravitational acceleration, $\mathbf{f}_B = \beta(T_{\text{ref}} - T)$ the buoyancy force, and $\mathbf{f}_{\text{EHD}} = qN_p\mathbf{E}$ the Coulomb force, assumed to be distributed over all gas particles via scattering. The electric current density $\mathbf{j}$ consists of drift, convection, and diffusion currents.

The system of coupled, nonlinear PDEs has to be solved for given initial and boundary conditions. Prior to discussing the latter, we summarize the global solution procedure. First, in a Gauss-Seidel-like approach, the solution is determined progressively for the block

$\phi - N_p$, then for the block $p - \mathbf{v}$ and finally for T. Because of the weak influence of each block to the preceding ones, only one iteration per time step is performed. Electrostatics equations are solved with nonlinear formulation to reach convergence (for details, see [2]) while Navier-Stokes block is solved via a SIMPLE-like projection method ($\lambda(\mathbf{v})$ being a coefficient depending on both the estimated velocity and the grid). Here we sketch how this iteration is built:

- ■ `until` $\int_\Omega (N_p^{(k-1)} e^{\phi^{(k,0)} - \phi^{(k,n)}} - N_p^{(k)}) < $ `tol.`
  - ● `until` $\|\phi^{(k,n-1)} - \phi^{(k,n)}\|_\infty < $ `tol.`
    - ▲ `solve` $-\nabla \cdot (\varepsilon\nabla\phi^{(k,n)}) = qN_p^{(k-1)} e^{\phi^{(k,0)} - \phi^{(k,n)}}$, `linearized around` $\phi^{(k,n-1)}$
  - ● `solve` $q\frac{\partial N_p^{(k)}}{\partial t} = -\nabla \cdot \left(\mathbf{j}(\phi^{(k,n)}, N_p^{(k)})\right)$
- ■ `solve momentum equation (4) for` $\mathbf{v}^{(0)}$
- ■ `until` $\int_\Omega \nabla \cdot \mathbf{v}^{(j)} < $ `tol.`
  - ● `solve` $-\nabla \cdot \left(\lambda(\mathbf{v}^{(j-1)})\nabla p^{(j)}\right) = \nabla \cdot \mathbf{v}^{(j-1)}$
  - ● `correct` $\mathbf{v}^{(j)} = \mathbf{v}^{(j-1)} - \lambda(\mathbf{v}^{(j-1)})\nabla p^{(j)}$
- ■ `solve temperature equation (5)`

2 Corona discharge boundary conditions

We restrict our discussion to the BC for N_p at the *corona* electrode, comparing four different BC types. For the rest of the boundaries, instantaneous recombination BC ($\mathbf{n} \cdot \nabla N_p = 0$) is applied at counter electrodes, while in all other cases well-known standard BCs can be used.

The first approach we present is the *natural condition*, namely imposing the normal flux j_n associated to (2) to be uniform; this approach is very accurate when geometry is symmetric and one knows the actual current from measurments, but has the drawback of being totally unpredictive. Nonetheless, this approach is sometimes used with arbitrary geometries, defining an *active surface* that emits the necessary current density. The generally accepted *Kaptsov's hypothesis* (see [5]) states that $E_n := \mathbf{E} \cdot \mathbf{n} = E_{\text{on}}$, namely the field remains constant at the (virtual) electrode once the corona discharge is triggered. A value for E_{on} can be computed from *Peek's law* (see e.g. [6], ch. 4) and allows to define the active region as the part of the boundary where $E_n > E_{\text{on}}$ holds.

For having a predictive condition, instead, one needs to somehow enforce a *constitutive law* linking
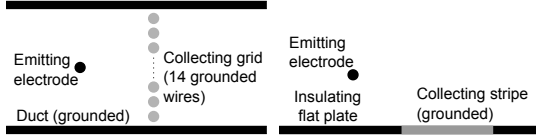
Fig. 1. Gometries from [4] (left) and from [3] (right).

Fig. 2. Comparison of the graphs on the $N_p - E_n$ plane defined by the constitutive relations $F_i(E_n, N_p) = 0$.

Fig. 3. IV-characteristic for the wire to grid (left) and wire to plate (right) geometries.

j_n or N_p with E_n. We choose to adopt the second, simpler formulation, namely to impose $F_i(E_n, N_p) = 0$ to be satisfied on the boundary. Our first approach, given in [1], is based on a simplified physical model of the virtual contact which takes into account charge carriers injected solely from the active surface (with a saturation current density $j_{sat}H(E_n - E_{on})$, where $H(\bullet)$ is the Heaviside step function), and backscattered carriers (with current density given by $-qN_pw$ at the contact, where w is a characteristic velocity). Neglecting diffusion current at the electrode, this approach can be interpreted as imposing the relation

$$F_1(E_n, N_p) = qN_p(bE_n - w) - j_{sat}H(E_n - E_{on}) = 0 \quad (6)$$

Choice for the parameters j_{sat} and w needs to guarantee that the injected charge can naturally force $E_n = E_{on}$, otherwise current density saturates to $j_n = j_{sat}$ and *space charge controlled current* (SCCC) regime is not reached anymore.

Our second approach is to model the boundary as an ideal *rectifying diode*, in which no ion density is flowing under the E_{on} treshold, while every N_p value is possible when $E_n = E_{on}$. Explicitly, this approach is equivalent to enforce the following:

$$F_2(E_n, N_p) = N_p \left(1 - \left(\frac{E_n}{E_{ons}}\right)^\beta\right) = 0 \quad (7)$$

$\beta \in [0, 1]$ being a smoothing factor. This relation strongly enforces both N_p to vanish in the other non active portion of the electrode, and E_n to match E_{on} in the active portion.

Our last approach assumes a constitutive relation which is a more regular version for the former one:

$$F_3(E_n, N_p) = N_p - N_{ref}\left(\exp\left(\frac{E_n}{E_{ref}}\right) + 1\right) = 0 \quad (8)$$

where N_{ref} and E_{ref} are a device-off ion density and a reference electric field. The choice of these two values can thus be made independently from the particular case (using e.g. air conductivity for N_{ref}).

3 Results and conclusions

As examples, a wire-to-grid geometry [4] and a wire-to-plate geometry [3] have been investigated (Fig. 1).

The former consists of a duct with a grounded grid in the middle (both collectors), and an emitter placed upstream. The E_{on} value is determined from the 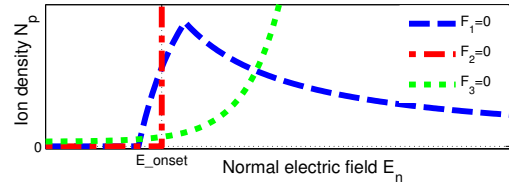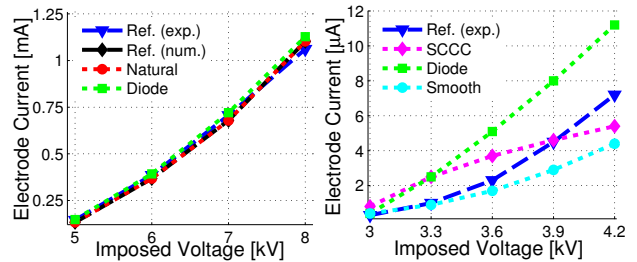experimental onset voltage (4 kV). Simulations show how the natural condition matches exactly the experimental value, and the iterative condition as in (7) still captures well the electrical behavior. One may thus consider that in cases like this, even when lacking measured currents, the ideal diode model is still appropriate.

The latter geometry has a heated plate with a collecting stripe and the emitter is lifted from the plate. As shown in Fig 3, this case is not as well reproduced as the former, due to the highly nonuniform E_n on the electrode. This issue may be solved with a parameter optimization, which has not yet been undertaken in the present study. The current, being the most influential parameter for for the fluid dynamics and thermal computing, was predicted with acceptable accuracy.

References

1. T. Christen and M. Seeger. Simulation of unipolar space charge controlled electric fields. *J. Electrostatics*, 65:11–20, 2007.
2. C. de Falco, J. W. Jerome, and R. Sacco. Quantum-corrected drift-diffusion models: Solution fixed point map and finite element approximation. *J.Comp.Phys.*, 228:1770–1789, 2009.
3. D. B. Go et al. Enhancement of external forced convection by ionic wind. *I.J. Heat Mass Transfer*, 51:6047–6053, 2008.
4. N. E. Jewell-Larsen et al. Modeling of corona-induced electrohydrodynamic flow with comsol multiphysics. In *Proc. of ESA Annual Meeting on Electrostatics*, 2008.
5. N. A. Kaptsov. *Elektricheskie Yavleniya v Gazakh i Vakuume*. OGIZ, Moskva, 1947.
6. H. J. White. *Industrial electrostatic precipitation*. Addison-Wesley, New York, 1963.